PAPER

Circuit Modeling Technique for Electrically-Very-Small Devices Based on Laurent Series Expansion of Self-/Mutual Impedances

Nozomi HAGA[†a)], ***Member and*** **Masaharu TAKAHASHI**[††b)], ***Fellow***

SUMMARY This paper proposes a circuit modeling technique for electrically-very-small devices, e.g. electrodes for intrabody communications, coils for wireless power transfer systems, high-frequency transformers, etc. The proposed technique is based on the method of moments and can be regarded as an improved version of the partial element equivalent circuit method.

key words: *equivalent circuit modeling, method of moments, impedance expansion method*

1. Introduction

Electrically-very-small devices are widely used for various wireless and wired systems. Typical examples include electrodes for intrabody communications [1], coils for wireless power transfer systems [2], high-frequency transformers, etc. It is well known that undesired resonances or radiations may occur at the usual operating frequencies of these devices, and they affect their operating characteristics or cause noises [3]. Therefore, these devices should be treated as problems of high-frequency electromagnetic fields even if they are much smaller than the wavelength.

Besides, the electromagnetic characteristics of electrically-very-small devices may be approximated by equivalent circuits. This approach has the benefits such that:

1. small-scale circuit models can easily be analyzed via theoretical approaches, which give us an insight on the operation mechanism of the devices;
2. the interaction between the electromagnetic fields and the non-linear electronic circuits can be analyzed only by importing the equivalent-circuit parameters into versatile circuit simulators.

In the previous studies, various circuit-modeling methods have been proposed, and they can be categorized into the following approaches:

1. those which derive analytical expressions for the circuit parameters by simplifying the problems [4], [5];
2. those which determine the parameters of assumed circuit models so that the frequency characteristics of the circuits fit to those obtained via existing electromagnetic simulators or measurements [6]–[8];
3. those which obtain the circuit parameters by discretizing the integral equations that hold true in the problems [9]–[11].

The first approach gives us a clear insight on how to determine the physical parameters. However, its applicable scope is limited in general. The second approach can be applied to various problems without complicated considerations involving Maxwell's equations. This means, however, that the physical meaning of the obtained circuit parameters is hard to interpret. This paper employs the third approach, which is well-balanced in terms of these points, and intends to establish a basis for a versatile circuit modeling technique.

The method described in [9], [10] is called the partial element equivalent circuit (PEEC) method, and is accepted in the fields such as power electronics. Several features of the PEEC method are the same as those of the method of moments (MoM) [12], which is well-established in the fields of antennas and propagation, because both of them are based on the same integral equations. The method proposed in this paper is based on the MoM, and at the same time, can be regarded as an extension of the PEEC method and superior to the conventional PEEC method in accuracy.

This paper is organized as follows. Section 2 derives the Laurent series expansion of the self-/mutual impedances between arbitrary basis functions, which is the basis of the proposed method. In addition, the physical meaning of the expanded expression is discussed. Section 3 deals with an example problem to demonstrate the proposed method and describes the relation between the proposed method and the PEEC method. Subsequently, Sect. 4 shows numerical examples to compare the results obtained via the PEEC method, the proposed method, and the induced electromotive force (EMF) method. Finally, Sect. 5 concludes this paper.

2. Laurent Series Expansion of Self-/Mutual Impedances between Arbitrary Basis Functions

As described before, the proposed modeling technique is based on the Laurent series expansion of the self-/mutual impedances in the MoM. Whereas the previous studies have derived the similar expressions for specific basis functions, this paper derives a general expression for arbitrary basis functions.

In Galerkin's MoM, the self-/mutual impedance be-

Manuscript received May 19, 2017.
Manuscript revised July 10, 2017.
Manuscript publicized August 14, 2017.

[†]The author is with the Graduate School of Science and Technology, Gunma University, Kiryu-shi, 376-8585 Japan.
[††]The author is with the Center for Frontier Medical Engineering, Chiba University, Chiba-shi, 263-8522 Japan.
a) E-mail: nozomi.haga@gunma-u.ac.jp
b) E-mail: omei@m.ieice.org

DOI: 10.1587/transcom.2017EBP3196

tween basis functions $\boldsymbol{F}_m(\boldsymbol{r})$ and $\boldsymbol{F}_n(\boldsymbol{r}')$ is given as follows [13]:

$$Z_{mn} = s\frac{\zeta}{4\pi c}\int_S\int_S \boldsymbol{F}_m(\boldsymbol{r})\cdot\boldsymbol{F}_n(\boldsymbol{r}')\frac{e^{-sR/c}}{R}dS'dS + \frac{1}{s}\frac{\zeta c}{4\pi}\int_S\int_S[\nabla\cdot\boldsymbol{F}_m(\boldsymbol{r})][\nabla'\cdot\boldsymbol{F}_n(\boldsymbol{r}')]\frac{e^{-sR/c}}{R}dS'dS, \tag{1}$$

where $s = j\omega$ is the complex angular frequency; ζ is the wave impedance; c is the speed of light; $\boldsymbol{r}$ is the observation point; $\boldsymbol{r}'$ is the source point; $R = |\boldsymbol{r} - \boldsymbol{r}'|$ is the distance between the observation and the source points; ∇ and ∇' are the vector differential operators with respect to $\boldsymbol{r}$ and $\boldsymbol{r}'$, respectively; and dS and dS' are the surface elements with respect to $\boldsymbol{r}$ and $\boldsymbol{r}'$, respectively. Besides, S is all the closed surfaces on conductors. The basis functions shall be frequency-independent real functions and shall satisfy the following condition:

$$\boldsymbol{F}_m(\boldsymbol{r})\cdot\hat{n} = 0, \quad \boldsymbol{r}\in S;\ m = 1,\ldots,N, \tag{2}$$

where $\hat{n}$ is the outward unit normal vector at $\boldsymbol{r}$ on S, i.e. the basis functions are tangential to S.

By expanding the exponential function in Eq. (1) into the Taylor series, we get the Laurent series expansion of Z_{mn} as follows:

$$Z_{mn} = \sum_{i=-1}^{\infty} s^i Z_{mn}^{(i)}, \tag{3}$$

where the coefficients for the respective powers are as follows:

$$Z_{mn}^{(-1)} = \frac{\zeta c}{4\pi}\int_S\int_S[\nabla\cdot\boldsymbol{F}_m(\boldsymbol{r})][\nabla'\cdot\boldsymbol{F}_n(\boldsymbol{r}')]\frac{1}{R}dS'dS, \tag{4}$$

$$Z_{mn}^{(0)} = 0, \tag{5}$$

$$Z_{mn}^{(i)} = \frac{(-1)^{i-1}\zeta}{(i-1)!4\pi c^i}\int_S\int_S \boldsymbol{F}_m(\boldsymbol{r})\cdot\boldsymbol{F}_n(\boldsymbol{r}')R^{i-2}dS'dS + \frac{(-1)^{i+1}\zeta}{(i+1)!4\pi c^i}\int_S\int_S[\nabla\cdot\boldsymbol{F}_m(\boldsymbol{r})][\nabla'\cdot\boldsymbol{F}_n(\boldsymbol{r}')]R^i dS'dS, \quad i\geq 1, \tag{6}$$

where the equality of Eq. (5) is proven in Appendix A.

It is notable that several low-order terms in Eq. (3) have explicit physical meanings. The lowest-order term $s^{-1}Z_{mn}^{(-1)}$ is equivalent to the impedance of the capacitance

$$C = \frac{1}{Z_{mn}^{(-1)}} = \left\{\frac{\zeta c}{4\pi}\int_S\int_S[\nabla\cdot\boldsymbol{F}_m(\boldsymbol{r})][\nabla'\cdot\boldsymbol{F}_n(\boldsymbol{r}')]\frac{1}{R}dS'dS\right\}^{-1}.$$

Similarly, the term $sZ_{mn}^{(1)}$ is equivalent to the impedance of the inductance

$$L = Z_{mn}^{(1)} = \frac{\zeta}{4\pi c}\int_S\int_S \boldsymbol{F}_m(\boldsymbol{r})\cdot\boldsymbol{F}_n(\boldsymbol{r}')\frac{1}{R}dS'dS + \frac{\zeta}{8\pi c}\int_S\int_S[\nabla\cdot\boldsymbol{F}_m(\boldsymbol{r})][\nabla'\cdot\boldsymbol{F}_n(\boldsymbol{r}')]R\,dS'dS,$$

where the first term in the right-hand side corresponds to Neumann's formula. Besides, the term $s^2Z_{mn}^{(2)}$ can be simplified as follows:

$$s^2Z_{mn}^{(2)} = -s^2\frac{\zeta}{6\pi c^2}\left[\int_S \boldsymbol{F}_m(\boldsymbol{r})\,dS\right]\cdot\left[\int_S \boldsymbol{F}_n(\boldsymbol{r}')\,dS'\right], \tag{7}$$

where the equality of Eq. (7) is proven in Appendix B. In particular, the self-impedance component $s^2Z_{mn}^{(2)}$ is equivalent to the radiation resistance of the infinitesimal dipole [14] with the length of

$$l = \left|\int_S \boldsymbol{F}_m(\boldsymbol{r})\,dS\right|.$$

It should be noted that the infinite series in Eq. (3) should be approximated by a finite series so that the residual error is sufficiently small. However, the required number of terms is expected to be small for the problems much smaller than the wavelength. The proposed method is hereinafter called the impedance expansion method (IEM).

3. Example Problem

As shown in Fig. 1, a straight wire with radius a and length $3l$ has feeding ports 1 and 2 at $z = l$ and $2l$, respectively. In this section, the self- and the mutual impedances between the two ports are formulated and the equivalent circuit is first derived by the PEEC method. Then, it is shown that the equivalent circuit by the IEM can be regarded as an extension of that by the PEEC method. Subsequently, they are compared with the reference solution by the EMF method.

3.1 Formulation by PEEC Method

The PEEC method models the problem by the LC circuit

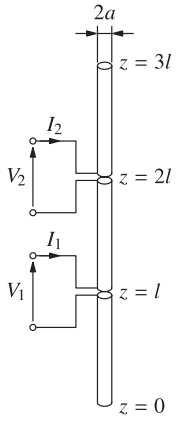

Fig. 1 A straight wire with two feeding ports.

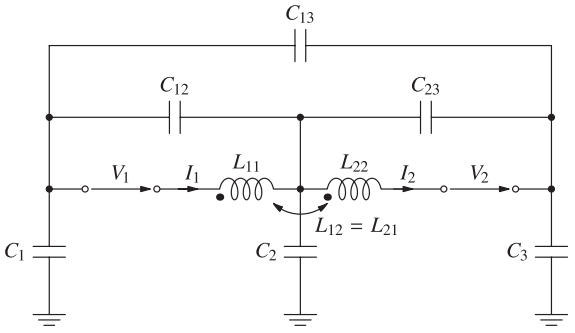

Fig. 2 Equivalent circuit by the PEEC method.

shown in Fig. 2. In the usual PEEC manner, inductive and capacitive elements are alternately placed so that their half segments overlap each other. In addition, the current and the charge distributions are assumed to be uniform on each inductive and capacitive element. In the present problem, two inductive basis functions ($m = 1, 2$)

$$f_m(z) = \begin{cases} 1, & |z - ml| < l/2 \\ 0, & \text{elsewhere} \end{cases} \tag{8}$$

and three capacitive basis functions ($m = 1, 2, 3$)

$$g_m(z) = \begin{cases} 1/l, & (m-1)l < z < ml \\ 0, & \text{elsewhere} \end{cases} \tag{9}$$

are assumed on the central axis of the wire, as shown in Fig. 3. It should be noted that the current and the charge distributions expanded by these functions do not satisfy the charge conservation law.

For a thin-wire structure, the expression for the self-/mutual inductances between the inductive basis functions [9], [10] can reduce to

$$L_{mn} = \frac{\zeta}{4\pi c} \int_0^{3l}\int_0^{3l} f_m(z)\, f_n(z') \frac{1}{R}\, dz'dz, \tag{10}$$

where

$$R = \sqrt{a^2 + (z - z')^2}. \tag{11}$$

By substituting Eq. (8) into Eq. (10) and performing the integrations, the self-inductances $L_{11} = L_{22}$ and the mutual inductances $L_{12} = L_{21}$ are calculated as follows:

$$L_{11} = \frac{\zeta l}{4\pi c}\left(2\,\mathrm{arsinh}\,\frac{l}{a} - \frac{2\sqrt{l^2+a^2}}{l} + \frac{2a}{l}\right), \tag{12}$$

$$L_{12} = \frac{\zeta l}{4\pi c}\left(2\,\mathrm{arsinh}\,\frac{2l}{a} - 2\,\mathrm{arsinh}\,\frac{l}{a} - \frac{\sqrt{4l^2+a^2}}{l} + \frac{2\sqrt{l^2+a^2}}{l} - \frac{a}{l}\right). \tag{13}$$

Similarly, the expression for the self-/mutual potential coefficients [9], [10] can reduce to

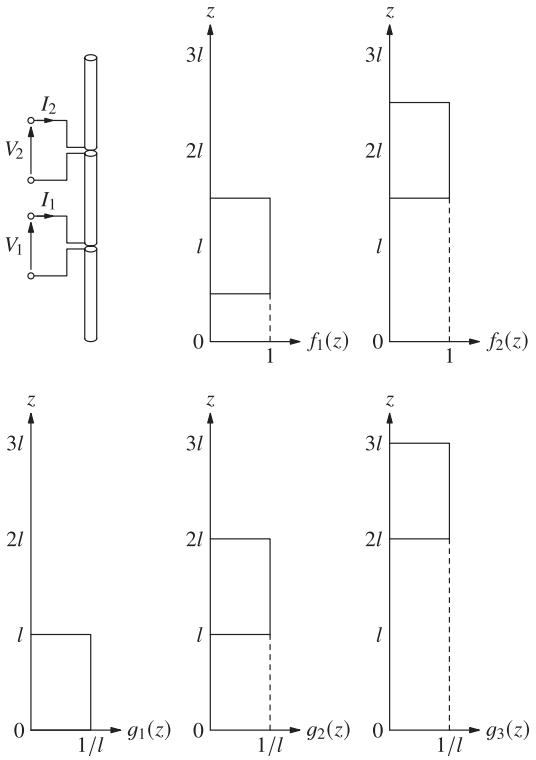

Fig. 3 Basis functions used in the PEEC method.

$$p_{mn} = \frac{\zeta c}{4\pi} \int_0^{3l}\int_0^{3l} g_m(z)\, g_n(z') \frac{1}{R}\, dz'dz, \tag{14}$$

where R is the same as that in Eq. (11). By substituting Eq. (9) into Eq. (14) and performing the integrations, the self-potential coefficients $p_{11} = p_{22} = p_{33}$ and the mutual potential coefficients $p_{12} = p_{21} = p_{23} = p_{32}$, $p_{13} = p_{31}$ are calculated as follows:

$$p_{11} = \frac{\zeta c}{4\pi l}\left(2\,\mathrm{arsinh}\,\frac{l}{a} - \frac{2\sqrt{l^2+a^2}}{l} + \frac{2a}{l}\right), \tag{15}$$

$$p_{12} = \frac{\zeta c}{4\pi l}\left(2\,\mathrm{arsinh}\,\frac{2l}{a} - 2\,\mathrm{arsinh}\,\frac{l}{a} - \frac{\sqrt{4l^2+a^2}}{l} + \frac{2\sqrt{l^2+a^2}}{l} - \frac{a}{l}\right), \tag{16}$$

$$p_{13} = \frac{\zeta c}{4\pi l}\left(3\,\mathrm{arsinh}\,\frac{3l}{a} - 4\,\mathrm{arsinh}\,\frac{2l}{a} + \mathrm{arsinh}\,\frac{l}{a} - \frac{\sqrt{9l^2+a^2}}{l} + \frac{2\sqrt{4l^2+a^2}}{l} - \frac{\sqrt{l^2+a^2}}{l}\right). \tag{17}$$

By using the obtained potential coefficients, the capacitances in Fig. 2 can be obtained as follows:

$$\begin{bmatrix} c_{11} & c_{12} & c_{13} \\ c_{21} & c_{22} & c_{23} \\ c_{31} & c_{32} & c_{33} \end{bmatrix} = \begin{bmatrix} p_{11} & p_{12} & p_{13} \\ p_{21} & p_{22} & p_{23} \\ p_{31} & p_{32} & p_{33} \end{bmatrix}^{-1}, \tag{18}$$

$$C_m = \sum_{n=1}^{3} c_{mn}, \quad C_{mn} = -c_{mn}. \tag{19}$$

By writing and solving the circuit equations of the equivalent circuit in Fig. 2, the self- and the mutual impedances are obtained as follows:

$$Z_{11} = Z_{22} = s^{-1}Z_{11}^{(-1)} + sZ_{11}^{(1)}, \tag{20}$$

$$Z_{12} = Z_{21} = s^{-1}Z_{12}^{(-1)} + sZ_{12}^{(1)}, \tag{21}$$

where

$$\begin{aligned} Z_{11}^{(-1)} &= p_{11} - p_{12} - p_{21} + p_{22} \\ &= \frac{\zeta c}{4\pi l}\left(-4\,\mathrm{arsinh}\,\frac{2l}{a} + 8\,\mathrm{arsinh}\,\frac{l}{a} \right. \\ &\quad \left. + \frac{2\sqrt{4l^2+a^2}}{l} - \frac{8\sqrt{l^2+a^2}}{l} + \frac{6a}{l}\right), \end{aligned} \tag{22}$$

$$\begin{aligned} Z_{12}^{(-1)} &= p_{12} - p_{13} - p_{22} + p_{23} \\ &= \frac{\zeta c}{4\pi l}\left(-3\,\mathrm{arsinh}\,\frac{3l}{a} + 8\,\mathrm{arsinh}\,\frac{2l}{a} \right. \\ &\quad - 7\,\mathrm{arsinh}\,\frac{l}{a} + \frac{\sqrt{9l^2+a^2}}{l} \\ &\quad \left. - \frac{4\sqrt{4l^2+a^2}}{l} + \frac{7\sqrt{l^2+a^2}}{l} - \frac{4a}{l}\right), \end{aligned} \tag{23}$$

$$Z_{11}^{(1)} = L_{11}, \tag{24}$$

$$Z_{12}^{(1)} = L_{12}. \tag{25}$$

3.2 Formulation by IEM

In the IEM, the current distributions are assumed at the central axis of the wire and expanded by piecewise linear basis functions ($m = 1, 2$)

$$f_m(z) = \begin{cases} \dfrac{l - |ml - z|}{l}, & |z - ml| < l \\ 0, & \text{elsewhere} \end{cases}, \tag{26}$$

as shown in Fig. 4. Besides, the charge distributions are expanded by the derivatives of the basis functions

$$\frac{\partial f_m(z)}{\partial z} = \begin{cases} \dfrac{ml - z}{|ml - z|l}, & |z - ml| < l \\ 0, & \text{elsewhere} \end{cases}. \tag{27}$$

It should be noted that the current and the charge distributions expanded by these functions automatically satisfy the charge conservation law.

For a thin-wire structure, Eqs. (4) and (6) can reduce to

$$Z_{mn}^{(-1)} = \frac{\zeta c}{4\pi}\int_0^{3l}\int_0^{3l} \frac{\partial f_m(z)}{\partial z}\frac{\partial f_n(z')}{\partial z'}\frac{1}{R}\,dz'dz, \tag{28}$$

$$\begin{aligned} Z_{mn}^{(i)} &= \frac{(-1)^{i-1}\zeta}{(i-1)!4\pi c^i}\int_0^{3l}\int_0^{3l} f_m(z)\, f_n(z')\, R^{i-2}dz'dz \\ &\quad + \frac{(-1)^{i+1}\zeta}{(i+1)!4\pi c^i}\int_0^{3l}\int_0^{3l} \frac{\partial f_m(z)}{\partial z}\frac{\partial f_n(z')}{\partial z'}\, R^i dz'dz, \\ &\qquad\qquad i \geq 1, \end{aligned} \tag{29}$$

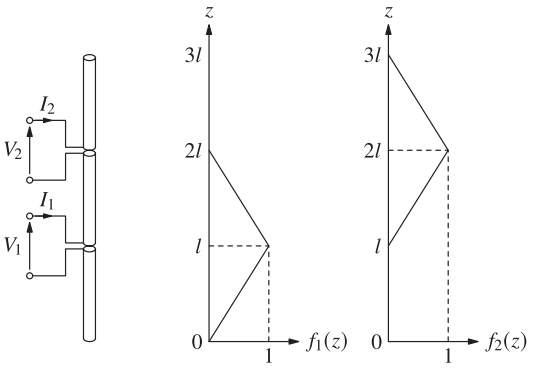

Fig. 4 Basis functions used in the IEM.

respectively, where R is the same as that in Eq. (11). By substituting Eqs. (26) and (27) into Eqs. (28) and (29) and ignoring the terms of $i \geq 3$, we get the following expressions for the self- and the mutual impedances:

$$Z_{11} = Z_{22} \simeq s^{-1}Z_{11}^{(-1)} + sZ_{11}^{(1)} + s^2Z_{11}^{(2)}, \tag{30}$$

$$Z_{12} = Z_{21} \simeq s^{-1}Z_{12}^{(-1)} + sZ_{12}^{(1)} + s^2Z_{12}^{(2)}, \tag{31}$$

where the expressions for $Z_{11}^{(-1)}$ and $Z_{12}^{(-1)}$ are the same as those in Eqs. (22) and (23) derived by the PEEC method; and the other components are as follows:

$$\begin{aligned} Z_{11}^{(1)} &= \frac{\zeta l}{4\pi c}\left(\frac{8l^2 - 6a^2}{3l^2}\,\mathrm{arsinh}\,\frac{2l}{a} \right. \\ &\quad - \frac{4l^2 - 12a^2}{3l^2}\,\mathrm{arsinh}\,\frac{l}{a} \\ &\quad - \frac{28l^2 - 5a^2}{9l^3}\sqrt{4l^2+a^2} \\ &\quad \left. + \frac{28l^2 - 20a^2}{9l^3}\sqrt{l^2+a^2} + \frac{5a^3}{3l^3}\right), \end{aligned} \tag{32}$$

$$\begin{aligned} Z_{12}^{(1)} &= \frac{\zeta l}{4\pi c}\left(\frac{9l^2 - 3a^2}{2l^2}\,\mathrm{arsinh}\,\frac{3l}{a} \right. \\ &\quad - \frac{16l^2 - 12a^2}{3l^2}\,\mathrm{arsinh}\,\frac{2l}{a} \\ &\quad + \frac{7l^2 - 21a^2}{6l^2}\,\mathrm{arsinh}\,\frac{l}{a} \\ &\quad - \frac{63l^2 - 5a^2}{18l^3}\sqrt{9l^2+a^2} \\ &\quad + \frac{56l^2 - 10a^2}{9l^3}\sqrt{4l^2+a^2} \\ &\quad \left. - \frac{49l^2 - 35a^2}{18l^3}\sqrt{l^2+a^2} - \frac{10a^3}{9l^3}\right), \end{aligned} \tag{33}$$

$$Z_{11}^{(2)} = Z_{12}^{(2)} = -\frac{\zeta l^2}{6\pi c^2}. \tag{34}$$

It is notable that the PEEC method and the IEM yield the same expressions for $Z_{11}^{(-1)}$ and $Z_{12}^{(-1)}$ because the charge distributions are assumed to be uniform across the intervals $[0, l]$, $[l, 2l]$, and $[2l, 3l]$ in both the methods, i.e. the charge distributions are expanded by the capacitive basis functions

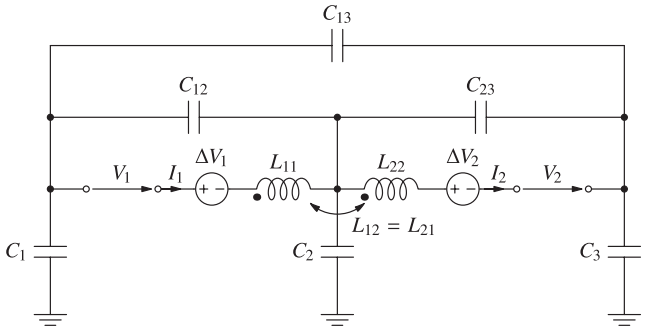

Fig. 5 Equivalent circuit by the IEM.

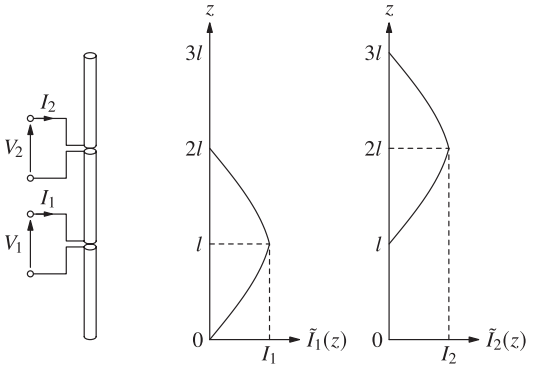

Fig. 6 Current distributions used in the EMF method.

expressed by Eq. (9) in the PEEC method whereas they are expanded by the derivative of the piecewise linear basis functions expressed by Eq. (27) in the IEM. By using this fact and introducing self- and mutual inductances

$$L_{11} = L_{22} = Z_{11}^{(1)} = Z_{22}^{(1)}, \tag{35}$$

$$L_{12} = L_{21} = Z_{12}^{(1)} = Z_{21}^{(1)}, \tag{36}$$

and dependent voltage sources

$$\Delta V_1 = s^2 Z_{11}^{(2)} I_1 + s^2 Z_{12}^{(2)} I_2, \tag{37}$$

$$\Delta V_2 = s^2 Z_{21}^{(2)} I_1 + s^2 Z_{22}^{(2)} I_2, \tag{38}$$

the self- and the mutual impedances expressed by Eqs. (30) and (31) can also be represented by the equivalent circuit shown in Fig. 5. From this viewpoint, the IEM can be regarded as an extension of the PEEC method, and its improved points are that:

1. the basis functions and their derivatives satisfy the charge conservation law;
2. the radiation loss is represented by the dependent voltage sources.

3.3 Formulation by EMF Method

In the orthodox manner of the EMF method, a set of sinusoidal current distributions ($m = 1, 2$)

$$\tilde{I}_m(z) = \begin{cases} I_m \dfrac{\sinh[s(l - |ml - z|)/c]}{\sinh(sl/c)}, & |z - ml| < l \\ 0, & \text{elsewhere} \end{cases}$$

are assumed on the central axis of the wire, as shown in Fig. 6.

The E_z component of the electric field generated by the current $\tilde{I}_1(z)$ is expressed as follows:

$$E_z(z) = \frac{\zeta I_1}{4\pi \sinh(sl/c)} \left[\frac{e^{-sR_0/c}}{R_0} - 2\cosh\left(\frac{sl}{c}\right) \frac{e^{-sR_1/c}}{R_1} + \frac{e^{-sR_2/c}}{R_2} \right],$$

where

$$R_m = \sqrt{a^2 + (z - ml)^2}, \quad m = 1, 2, 3.$$

The self- and the mutual impedances are expressed by the following integrals:

$$Z_{11} = Z_{22} = -\frac{1}{|I_1|^2} \int_0^{2l} E_z(z)\, \tilde{I}_1^*(z)\, dz, \tag{39}$$

$$Z_{12} = Z_{21} = -\frac{1}{I_1 I_2^*} \int_l^{3l} E_z(z)\, \tilde{I}_2^*(z)\, dz, \tag{40}$$

where the superscript asterisk denotes the complex conjugate.

By expanding the integrands into the Laurent series, ignoring the terms of $i \geq 3$, and integrating the remaining terms, we get the following expressions for the self- and the mutual impedances:

$$Z_{11} = Z_{22} \simeq s^{-1} Z_{11}^{(-1)} + s Z_{11}^{(1)} + s^2 Z_{11}^{(2)}, \tag{41}$$

$$Z_{12} = Z_{21} \simeq s^{-1} Z_{12}^{(-1)} + s Z_{12}^{(1)} + s^2 Z_{12}^{(2)}, \tag{42}$$

where the expressions for $Z_{11}^{(-1)}$ and $Z_{12}^{(-1)}$ are the same as those in Eqs. (22) and (23) derived by the PEEC method and the IEM; the expressions for $Z_{11}^{(2)}$ and $Z_{12}^{(2)}$ are the same as those in Eq. (34) derived by the IEM; and the other components are as follows:

$$Z_{11}^{(1)} = \frac{\zeta l}{4\pi c} \left(-\frac{4}{3} \operatorname{arsinh} \frac{2l}{a} + \frac{8}{3} \operatorname{arsinh} \frac{l}{a} + \frac{10l^2 + a^2}{9l^3} \sqrt{4l^2 + a^2} - \frac{28l^2 + 4a^2}{9l^3} \sqrt{l^2 + a^2} + \frac{6l^2 + a^2}{3l^3} a \right), \tag{43}$$

$$Z_{12}^{(1)} = \frac{\zeta l}{4\pi c} \left(-\frac{7}{2} \operatorname{arsinh} \frac{3l}{a} + \frac{20}{3} \operatorname{arsinh} \frac{2l}{a} - \frac{17}{6} \operatorname{arsinh} \frac{l}{a} + \frac{30l^2 + a^2}{18l^3} \sqrt{9l^2 + a^2} - \frac{38l^2 + 2a^2}{9l^3} \sqrt{4l^2 + a^2} + \frac{58l^2 + 7a^2}{18l^3} \sqrt{l^2 + a^2} - \frac{6l^2 + 2a^2}{9l^3} a \right). \tag{44}$$

In other words, the only difference between the IEM and the EMF method is in the impedance components proportional to s. By introducing the inductances and the dependent voltage sources similar to those expressed by Eqs. (35)–(38), the self- and the mutual impedances expressed by Eqs. (41) and (42) can also be represented by the equivalent circuit shown in Fig. 5.

4. Numerical Examples

This section discusses numerical examples with the values of $a = 1.5$ mm and $l = 75$ mm. The capacitances obtained by all the methods are the same because the expressions for the self- and the mutual impedances proportional to s^{-1} are also the same. Their numerical values are as follows:

$$C_1 = C_3 = 933.0174 \text{ fF}, \qquad C_2 = 799.3008 \text{ fF},$$
$$C_{12} = C_{23} = 216.6863 \text{ fF}, \qquad C_{13} = 45.40740 \text{ fF}.$$

On the other hand, the expressions for the inductances by the respective methods are different each other. Table 1 compares the numerical values of the self- and the mutual in-

Table 1 Self- and mutual inductances (Unit: [nH]).

Parameter	PEEC	IEM	EMF
$L_{11} = L_{22}$	54.37605	36.60338	32.75083
$L_{12} = L_{21}$	10.24833	15.02211	15.56670

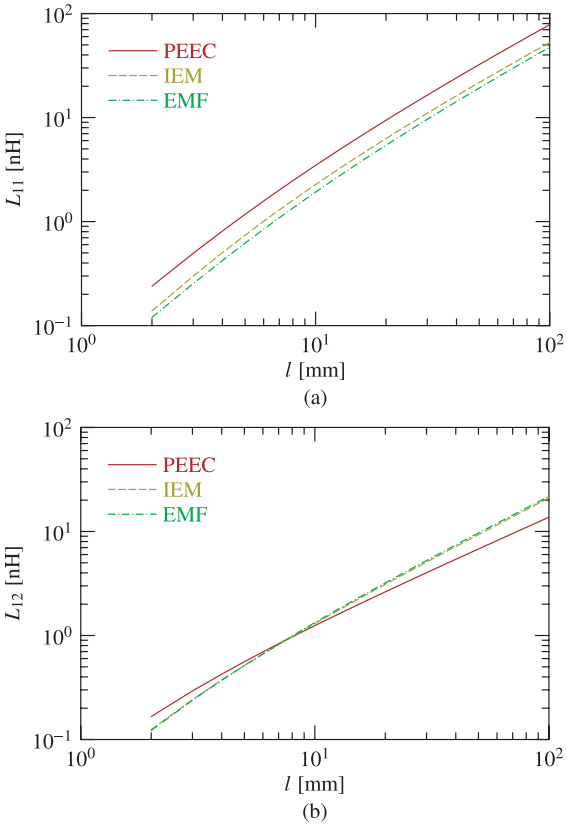

Fig. 7 Self- and mutual inductances: (a) L_{11}, (b) L_{12}.

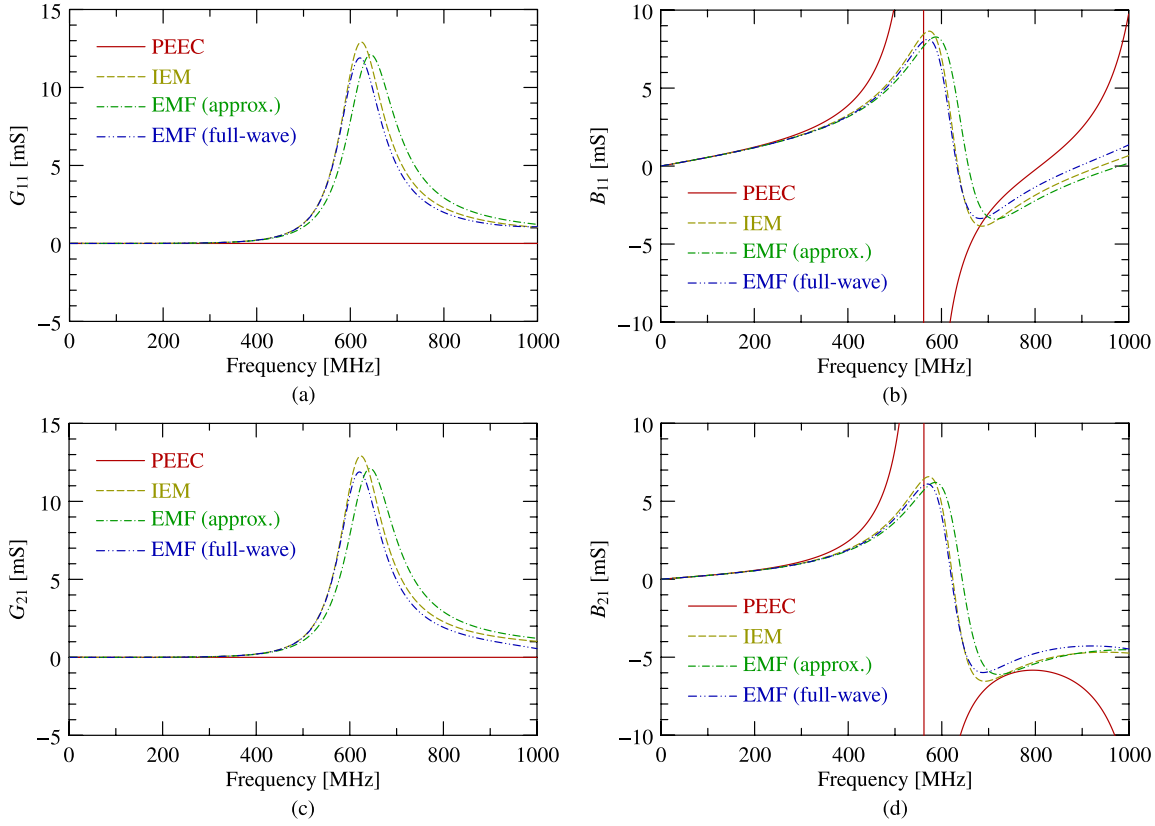

Fig. 8 Self- and mutual admittances: (a) G_{11}, (b) B_{11}, (c) G_{21}, (d) B_{21}.

ductances obtained by the three methods. In addition, Fig. 7 plots (a) the self- and (b) the mutual inductances as functions of l. Whereas those obtained by the IEM and the EMF method are comparable, those obtained by the PEEC method are considerably different. This is most likely because the shapes of the basis functions for the PEEC method are significantly different from those for the other methods, as shown in Figs. 3, 4, and 6. In particular, each basis function for the PEEC method concentrates on the length l whereas those for the other methods are distributed to the length $2l$. This is likely the reason why the self-inductance by the PEEC method are larger than the others. Besides, the basis functions for the PEEC method do not overlap each other in contrast to those for the other methods. In consequence, the trends of the mutual inductance by the PEEC method are different from the others.

Besides, the impedance components proportional to s^2, which are not defined in the PEEC method, are obtained by the IEM and the EMF method as $Z_{11}^{(2)} = Z_{12}^{(2)} = Z_{21}^{(2)} = Z_{22}^{(2)} = -1.2508654 \times 10^{-18}\ \Omega \cdot \mathrm{s}^2$.

Subsequently, the frequency characteristics of the equivalent circuits are discussed. As described previously, all methods yield the same impedance components proportional to s^{-1}. Because they are dominant at low frequencies, it is difficult to discuss the difference in the self- and the mutual impedances. Instead, the self- and the mutual admittances defined by

$$\begin{bmatrix} Y_{11} & Y_{12} \\ Y_{21} & Y_{22} \end{bmatrix} = \begin{bmatrix} Z_{11} & Z_{12} \\ Z_{21} & Z_{22} \end{bmatrix}^{-1} \tag{45}$$

are discussed.

Figure 8 plots (a) the real and (b) the imaginary parts of Y_{11} and (c) the real and (d) the imaginary parts of Y_{21}. The lines denoted by "EMF (approx.)" indicate the approximate solution by using Eqs. (41) and (42). On the other hand, the lines denoted by "EMF (full-wave)" indicate the reference solution by Eqs. (41) and (42), in which integrals were numerically calculated by using the tanh-sinh quadrature [15]. The results by the IEM and the approximated EMF method reasonably agree with those by the full-wave EMF method, whereas the results by the PEEC method are considerably different from the other results. This is mainly because the impedance components proportional to s^2, which represent the radiation loss, are not modeled in the PEEC method. The slight difference between the results by the IEM and the approximated EMF method is only due to the slight difference in the self- and the mutual inductances. Adittionally, the slight difference between the results by the approximated and the full-wave EMF methods is because the impedance components being proportional to s^3 and higher-order terms are ignored in the approximate solution.

5. Conclusion

In this paper, the basic theory and numerical examples of the impedance expansion method (IEM), which is a circuit modeling technique for electrically-very-small devices based on the MoM, are described.

Section 2 derived the Laurent series expansion of the self-/mutual impedances between arbitrary frequency-independent basis functions. It was also shown that the impedance components, which are proportional to the powers of the complex angular frequency, namely, s^{-1}, s, and s^2, correspond to the impedance of a capacitor, that of an inductor, and the radiation resistance of an infinitesimal dipole, respectively.

Section 3 showed that the equivalent circuit obtained by IEM can be regarded an extension of that obtained by the PEEC method. Section 4 showed that IEM is superior to the conventional PEEC method in terms of accuracy and is comparable to the EMF method.

Incidentally, this paper has not described how to realize the dependent voltage sources, which are proportional to s^2, in versatile circuit simulators. This can, however, be achieved by approximating the equivalent circuit using only passive elements. The details will be discussed in further studies. In addition, practical problems including the IBC and the WPT systems will be investigated as well.

References

[1] T.G. Zimmerman, "Personal area networks: Near-field intra-body communication," IBM Syst. J., vol.35, nos.3-4, pp.609–617, 1996.
[2] A. Karalis, J.D. Joannopoulos, and M. Soljačić, "Efficient wireless non-radiative mid-range energy transfer," Annals of Physics, vol.323, pp.34–48, 2008.
[3] R. Redl, "Electromagnetic environmental impact of power electronics equipment," Proc. IEEE, vol.89, no.6, pp.926–938, June 2001.
[4] R. Xu, W.C. Ng, and H. Zhu, "Equation environment coupling and interference on the electric-field intrabody communication channel," IEEE Trans. Biomed. Eng., vol.59, no.7, pp.2051–2059, July 2012.
[5] A. Massarini and M.K. Kazimierczuk, "Self-capacitance of inductors," IEEE Trans. Power Electron., vol.12, no.4, pp.671–676, July 1997.
[6] S. Igo, A. Fujiwara, and M. Taki, "Equivalent circuit of an intra-body communication device in consideration of human body resonance," IEICE Trans. Commun. (Japanese edition), vol.J95-B, no.9 pp.1090–1097, Sept. 2012.
[7] N. Inagaki and S. Hori, "Characterization of wireless connection systems of resonant method based on even and odd mode reactance functions and the image impedance," IEICE Trans. Commun. (Japanese edition), vol.J94-B, no.9, pp.1076–1085, Sept. 2011.
[8] H.Y. Lu, J.G. Zhu, and S.Y. R. Hui, "Experimental determination of stray capacitances in high frequency transformers," IEEE Trans. Power Electron., vol.18, no.5, pp.1105–1112, Sept. 2003.
[9] A.E. Ruehli, "Equivalent circuit models for three-dimensional multiconductor systems," IEEE Trans. Microw. Theory Techn., vol.22, no.3, pp.216–221, March 1974.
[10] H. Heeb and A.E. Ruehli, "Three-dimensional interconnect analysis using partial element equivalent circuits," IEEE Trans. Circuits Syst. I, Fundam. Theory Appl., vol.39, no.11, pp.974–982, Nov. 1992.
[11] N. Haga, K. Saito, M. Takahashi, and K. Ito, "Proper derivation of equivalent-circuit expressions of intra-body communication channels using quasi-static field," IEICE Trans. Commun., vol.E95-B, no.1, pp.51–59, Jan. 2012.
[12] R.F. Harrington, Field Computation by Moment Methods, Macmillan, New York, NY, USA, 1965.
[13] M.A. Tilston and K.G. Balmain, "On the suppression of asymmetric artifacts arising in an implementation of the thin-wire method of

moments," IEEE Trans. Antennas Propag., vol.38, no.2, pp.281–285, Feb. 1990.

[14] C.A. Balanis, Antenna Theory: Analysis and Design, 4th ed., John Wiley Sons, Hoboken, NJ, USA, 2016.

[15] H. Takahasi and M. Mori, "Double exponential formulas for numerical integration," Publ. Research Inst. Math. Sci., vol.9, no.3, pp.721–741, Kyoto Univ., 1974.

Appendix A: Proof of Eq. (5)

By expanding the exponential function in Eq. (1) into the Taylor series and taking the coefficient for s^0, we get the following expression for $Z_{mn}^{(0)}$:

$$\begin{aligned} Z_{mn}^{(0)} &= \frac{\zeta}{4\pi}\int_S\int_S [\nabla\cdot\boldsymbol{F}_m(\boldsymbol{r})][\nabla'\cdot\boldsymbol{F}_n(\boldsymbol{r}')]\,dS'dS \\ &= \frac{\zeta}{4\pi}\left[\int_S \nabla\cdot\boldsymbol{F}_m(\boldsymbol{r})\,dS\right]\left[\int_S \nabla'\cdot\boldsymbol{F}_n(\boldsymbol{r}')\,dS'\right]. \end{aligned}$$

According to the surface divergence theorem, the integrals in the right-hand side are zero because $\boldsymbol{F}_m(\boldsymbol{r})$ and $\boldsymbol{F}_n(\boldsymbol{r}')$ are tangential to the closed surface S. Therefore, we have equality of Eq. (5). □

Appendix B: Proof of Eq. (7)

By substituting $i = 2$ into Eq. (6), we get the following expression for $Z_{mn}^{(2)}$:

$$\begin{aligned} Z_{mn}^{(2)} &= -\frac{\zeta}{4\pi c^2}\int_S\int_S \boldsymbol{F}_m(\boldsymbol{r})\cdot\boldsymbol{F}_n(\boldsymbol{r}')\,dS'dS \\ &\quad -\frac{\zeta}{24\pi c^2}\int_S\int_S [\nabla\cdot\boldsymbol{F}_m(\boldsymbol{r})][\nabla'\cdot\boldsymbol{F}_n(\boldsymbol{r}')]R^2\,dS'dS. \end{aligned} \tag{A·1}$$

First, the following equality is proven:

$$\begin{aligned} &\int_S\int_S [\nabla\cdot\boldsymbol{F}_m(\boldsymbol{r})][\nabla'\cdot\boldsymbol{F}_n(\boldsymbol{r}')]R^2\,dS'dS \\ &\qquad = -2\int_S\int_S \boldsymbol{F}_m(\boldsymbol{r})\cdot\boldsymbol{F}_n(\boldsymbol{r}')\,dS'dS. \end{aligned} \tag{A·2}$$

According to the following relations

$$\begin{aligned} &\nabla'\cdot[\boldsymbol{F}_n(\boldsymbol{r}')R^2] = [\nabla'\cdot\boldsymbol{F}_n(\boldsymbol{r}')]R^2 + \boldsymbol{F}_n(\boldsymbol{r}')\cdot(\nabla'R^2), \\ &\nabla'R^2 = -2(\boldsymbol{r}-\boldsymbol{r}'), \end{aligned}$$

we have equality of

$$[\nabla'\cdot\boldsymbol{F}_n(\boldsymbol{r}')]R^2 = \nabla'\cdot[\boldsymbol{F}_n(\boldsymbol{r}')R^2] + 2\boldsymbol{F}_n(\boldsymbol{r}')\cdot(\boldsymbol{r}-\boldsymbol{r}').$$

By substituting this into the left-hand side of Eq. (A·2) and using the surface divergence theorem, we get

$$\mathrm{LHS} = 2\int_S \boldsymbol{F}_n(\boldsymbol{r}')\cdot\left\{\int_S [\nabla\cdot\boldsymbol{F}_m(\boldsymbol{r})]\,\boldsymbol{r}\,dS\right\}dS'. \tag{A·3}$$

Now, the integral in the curly brackets can be decomposed into the Cartesian components as follows:

$$\begin{aligned} &\int_S [\nabla\cdot\boldsymbol{F}_m(\boldsymbol{r})]\,\boldsymbol{r}\,dS = \hat{x}\int_S [\nabla\cdot\boldsymbol{F}_m(\boldsymbol{r})]\,x\,dS \\ &\quad + \hat{y}\int_S [\nabla\cdot\boldsymbol{F}_m(\boldsymbol{r})]\,y\,dS + \hat{z}\int_S [\nabla\cdot\boldsymbol{F}_m(\boldsymbol{r})]\,z\,dS. \end{aligned} \tag{A·4}$$

Because

$$\begin{aligned} \nabla\cdot[\boldsymbol{F}_m(\boldsymbol{r})\,x] &= [\nabla\cdot\boldsymbol{F}_m(\boldsymbol{r})]\,x + \boldsymbol{F}_m(\boldsymbol{r})\cdot(\nabla x) \\ &= [\nabla\cdot\boldsymbol{F}_m(\boldsymbol{r})]\,x + \boldsymbol{F}_m(\boldsymbol{r})\cdot\hat{x}, \end{aligned}$$

we have equality of

$$[\nabla\cdot\boldsymbol{F}_m(\boldsymbol{r})]\,x = \nabla\cdot[\boldsymbol{F}_m(\boldsymbol{r})\,x] - \boldsymbol{F}_m(\boldsymbol{r})\cdot\hat{x}. \tag{A·5}$$

Similarly,

$$[\nabla\cdot\boldsymbol{F}_m(\boldsymbol{r})]\,y = \nabla\cdot[\boldsymbol{F}_m(\boldsymbol{r})\,y] - \boldsymbol{F}_m(\boldsymbol{r})\cdot\hat{y}, \tag{A·6}$$

$$[\nabla\cdot\boldsymbol{F}_m(\boldsymbol{r})]\,z = \nabla\cdot[\boldsymbol{F}_m(\boldsymbol{r})\,z] - \boldsymbol{F}_m(\boldsymbol{r})\cdot\hat{z}. \tag{A·7}$$

By substituting Eqs. (A·5)–(A·7) into Eq. (A·4) and using the surface divergence theorem, we get

$$\int_S [\nabla\cdot\boldsymbol{F}_m(\boldsymbol{r})]\,\boldsymbol{r}\,dS = -\int_S \boldsymbol{F}_m(\boldsymbol{r})\,dS. \tag{A·8}$$

By substituting Eq. (A·8) into Eq. (A·3), the equality of Eq. (A·2) is proven:

$$\mathrm{LHS} = -2\int_S\int_S \boldsymbol{F}_n(\boldsymbol{r}')\cdot\boldsymbol{F}_m(\boldsymbol{r})\,dS'dS = \mathrm{RHS}.$$

Finally, by substituting Eq. (A·2) into Eq. (A·1), Eq. (7) is derived as follows:

$$\begin{aligned} Z_{mn}^{(2)} &= -\frac{\zeta}{6\pi c^2}\int_S\int_S \boldsymbol{F}_m(\boldsymbol{r})\cdot\boldsymbol{F}_n(\boldsymbol{r}')\,dS'dS \\ &= -\frac{\zeta}{6\pi c^2}\left[\int_S \boldsymbol{F}_m(\boldsymbol{r})\,dS\right]\cdot\left[\int_S \boldsymbol{F}_n(\boldsymbol{r}')\,dS'\right]. \end{aligned}$$

□

Nozomi Haga was born in Yamagata, Japan, in January 1985. He received the B.E., M.E., and D.E. degrees from Chiba University, Chiba, Japan, in 2007, 2009, and 2012, respectively. He is currently an Assistant Professor at Gunma University, Gunma, Japan. His main interests have been electrically small antennas and evaluation of body-centric wireless communication channels. He received the Young Researcher Encouraging Award of the IEICE Technical Committee on Antennas and Propagation in 2012. He is a member of the Institute of Electrical and Electronics Engineers (IEEE).

Masaharu Takahashi was born in Chiba, Japan, in December 1965. He received the B.E. degree in electrical engineering from Tohoku University, Miyagi, Japan, in 1989, and the M.E. and D.E. degrees in electrical engineering from the Tokyo Institute of Technology, Tokyo, Japan, in 1991 and 1994, respectively. From 1994 to 1996, he was a Research Associate, and from 1996 to 2000, an Assistant Professor with the Musashi Institute of Technology, Tokyo, Japan. From 2000 to 2004, he was an Associate Professor with the Tokyo University of Agriculture and Technology, Tokyo, Japan. He is currently an Associate Professor with the Research Center for Frontier Medical Engineering, Chiba University, Chiba, Japan. His main interests are electrically small antennas, planar array antennas, and EM compatibility. He was the recipient of the 1994 IEEE Antennas and Propagation Society (IEEE AP-S) Tokyo Chapter Young Engineer Award.